Variant and invariant features characterizing natural and reverse whole-body pointing movements

Enrico Chiovetto[1,2], Laura Patanè[2,3] and Thierry Pozzo[2,4,5]

1- Section for Computational Sensomotorics, Department of Cognitive Neurology, Hertie Institute for Clinical Brain Research, Centre for Integrative Neuroscience, University Clinic Tübingen, Tübingen, Germany

2- Department of Robotics, Brain and Cognitive Sciences, Italian Institute of Technology, Via Morego 30, 16163 Genova, Italy

3-Department of Communication, Computer and System Sciences - University of Genoa, Via dell' Opera Pia 13, 16145 Genova, Italy

4- Institut Universitaire de France, Université de Bourgogne, Dijon, Campus Universitaire, UFR STAPS, BP 27877, F-21078 Dijon, France

5- INSERM, U887, Motricité-Plasticité, Dijon, F-21078, France

Corresponding author: Dr. Enrico Chiovetto, Section for Computational Sensomotorics, Department of Cognitive Neurology, Hertie Institute for Clinical Brain Research, Frondsbergstrasse 23, 72070 Tübingen, Germany. Email: enrico.chiovetto@klinikum.uni-tuebingen.de

Keywords: Reverse whole-body pointing movements, coordination, principal component analysis, EMG, non-negative matrix factorization, multi-joint coordination

Abstract

Previous investigations showed that kinematics and muscle activity associated with natural whole-body movements along the gravity direction present modular organizations encoding specific aspects relative to both the motor plans and the motor programs underlying movement execution. It is however still unknown if such modular structures characterize also the reverse movements, when the displacement of a large number of joints is required to take the whole body back to a standing initial posture. To study what motor patterns are conserved across the reversal of movement direction, principal component analysis and non-negative matrix factorization were therefore applied respectively to the time series describing the temporal evolution of the elevation angles associated with all the body links and to the electromyographic signals of both natural and reverse whole-body movements. Results revealed that elevation angles where highly co-varying in time and that, despite some differences in the global parameters characterizing the different movements (indicating differences in high-level variable associated with the selected motor plans), the level of joint co-variation did not change across movement direction. In contrast, muscle organization of the forward whole-body pointing tasks was found to be different with respect to that characterizing the reverse movements. Such results agree with previous findings, according to which the central nervous system exploits, dependently on the direction of motion, different motor plans for the execution of whole-body movements. However, in addition, this study shows how such motor plans are translated into different muscle strategies that equivalently assure a high level of co-variation in the joint space.

Introduction

Movement accomplishment involves two kinds of variables: context-dependent and invariant variables. Those movement parameters that change the least under multiple kinds of movement transformation (such as translations, rotations or scaling in space) are usually referred to as motor patterns. Specific motor patterns were found characterizing, for instance, point-to-point arm movements (Morasso, 1981; Soechting and Flanders, 1991), handwriting tasks (Lacquaniti 1989; Polyakov et al, 2009) and locomotion (Ivanenko et al, 2004). Other investigations (Berret et al. 2009; Thomas et al. 2005) have shown that whole-body pointing (WBP) movements to reach a target from a standing position are organized according to a single coordinative structure in the space of the elevation angles, to assure simultaneous forward displacement of the global centre of mass (CoM) and hand trajectory formation.

Conversely, little is known about the motor patterns characterizing the reverse movements, when the displacement of a large number of joints is required to take the whole body back to a standing initial posture. In this case, indeed, the mechanical and sensory contexts result profoundly modified, mainly because of the different contribution of gravity to the dynamics of the movement. It makes therefore sense questioning about what motor patterns are conserved across the reversal of movement direction. Previous investigations characterizing sit-to-stand (STS) and the back-to-sit (BTS) motor tasks (see Papaxanthis et al. 2003) revealed general differences between the forward and return movements. Movement duration was significantly longer for downward compared with upward movements and also the shape of the velocity profiles changed: the relative acceleration duration (acceleration duration divided by movement duration during the vertical motion) was smaller for the upward compared with the downward displacement. Such considerations referred however more to

high- rather than to low-level movement variables (Lockhart and ting, 2007; Tresch, 2007), so that no information of inter-joint coordination could be retrieved from the analysis.

The kinematic behavior characterizing reverse WBP movements cannot be given for granted and many different possible strategies may be expected to regulate joint coordination. The two tasks are indeed drastically different. During the downward movement the motor goal is twofold: one has to point the target with the fingers (pointing sub-task) while balance has to be maintained (postural sub-task). During the returning movement instead, the task is mainly postural, as there is not target to point anymore and one has only to assume an upright standing position. Therefore, whereas strict coordination was found during downward movements (Berret and al. 2009), the subsequent return to the upright standing position might thus be obtained for instance by means of separate co-variation of the two groups of joints to make the relative body links (respectively those of the arms and those of the trunk plus lower-body) assume a vertical orientation in two consecutive moments.

In this study, we compared the kinematics and electromyographic (EMG) data of a natural WBP with that of the subsequent movement accomplished to return back to the initial standing position. Principal component analysis was applied to the time series describing the temporal evolution of the elevation angles associated with all the body links. Non-negative matrix factorization was moreover applied to the electromyographic signals. Results revealed that elevation angles where highly co-varying in time and that, despite some differences in the global parameters characterizing the different movements (i.e. differences regarding high-level variable associated with the selected motor plans), the level of joint co-variation did not change across movement direction. Differently, muscle organization of the forward whole-body pointing tasks was found to be different with respect to that characterizing the opposite movements. Such results agree with previous findings, according to which the central nervous system (CNS) exploits, dependently on the direction of motion, different motor

plans for the execution of whole-body movements. However, in addition, this study shows how such motor plans are translated into different muscle strategies that equivalently assure a high level of co-variation in the joint space.

Materials and Methods

Participants

Twelve healthy male subjects (ages 29 ± 4 years, mass 74 ± 9 kg, height 1.77 ± 0.07 m), participated voluntarily to the experiment. All subjects were in good health condition and had no previous history of neuromuscular disease. The experiment conformed to the declaration of Helsinki and informed consent was obtained from all the participants according to the protocol of the local ethical committee.

Protocol

Participants were required to perform a series of whole-body pointing movements toward a target located in front of them (forward movements, F), followed by backward movements to return to the initial standing position (returning movements, R). The target was a wooden dowel (45 cm long, 3 cm of diameter) positioned horizontally with respect to the ground, parallel to the subjects' coronal plane and with its centre intersecting the subjects' sagittal plane. For each participant, the two extremities of the dowel had a vertical distance from the ground equal to 25% of their body height. Two horizontal target distances (measured starting from the distal end of the participants' great toe) were tested: the first one (D1) corresponded to 15% of participants' height, the second one (D2) to 30%. Participants started from an upright standing position with their hands initially located at the

external side of the thighs. All movement, that were assumed to be symmetrical (Kaminski 2007), were performed in the sagittal plane, with each side of the body moving together. After verbal instruction that data recording had started, participants had to point to the target with both the index fingers at a comfortable velocity (not too slow or too fast to induce loss of balance). At the end of the pointing movement, they had to stand still on the final pointing position for about two seconds, keeping the fingers close to the extremities of the bar. They had then to return back to the initial upright position. Target accuracy was not the primary constraint during the experiments and no instruction was given to the participants regarding the strategy to follow to accomplish the task. Forward and return movements were considered separately in the analysis. Each subject performed one block of six valid trial repetitions for each target distance.

Apparatus

Movement kinematics was monitored by means of a Vicon (Oxford, UK) motion capture system. The temporal positions of eleven passive reflective markers attached to the right side of the participant's body were recorded during trial executions. Markers were attached to the lower limb (fifth metatarsophalangeal joint of the foot, lateral malleolus, knee interstitial joint space (lateral condyle of the femur), greater trochanter, iliac crest), arm (the acromion process, lateral epicondyle of the humerus, the styloid process and the tip of the index finger) and head (external canthus of the eye and auditory meatus). This marker configuration allowed schematizing the human body as a multi-joint system made of seven segments (as depicted in Fig. 1): head, trunk (thorax plus abdomen-pelvis), thighs (as a single segment), shanks, feet, upper arms and forearms. Electromyographic activity was monitored by means of an Aurion (Milan, Italy) wireless electromyographic system. EMG data were amplified (gain of 1000), band-pass filtered (10 Hz high-pass and 1 KHz low-pass) and digitized at

1000 Hz. Up to twenty-four different muscles from the right hemibody of each subject were simultaneously recorded: tibialis anterior (Tib), soleus (Sol), peroneus (Per), gastrocnemius lateralis (Gast), vastus lateralis (VL), biceps femoris (BF), vastus medialis (VM), semitendinosus (ST), rectus femoris (RF), semimembranosus (SM), adductor longus (AL), erector spinae (ES, with the electrodes over the longissimus thoracis at the level of the T8 spinal segment), rectus abdominis (RA), gluteus maximus (GM), internal oblique (OI), latissimus dorsi (LD), serratus anterior (Ser), anterior deltoid (DA), posterior deltoid (DP), pectoralis superior (Pect), rhomboid major (Rho), biceps brachii (Bic, short head), triceps brachii (Tri, lateral head) and brachioradialis muscle (Bra). The functional role of each single muscle and the right placement of the electrodes were tested by making subjects perform both isometric and free movements (Kendall et al., 2005).

Data collection and processing

Kinematic data were recorded at a sampling frequency of 100 Hz. They were analysed off-line using customized software written in Matlab (Mathworks, Natick, MA). Before any kind of analysis they were low-pass filtered (Butterworth filter, cut-off frequency of 20 Hz). Markers' velocities and accelerations and were obtained as first and second order derivatives of their spatial positions. Based on the multi-link model described above, the position of the global body centre of mass (CoM) was computed by means of standard methods and by using statistical anthropometric data (Winter 1990). The model and the method used to estimate the whole-body CoM trajectory were already validated in previous studies (Chiovetto et al., 2010; Stapley et al., 1999). Marker positions were used to compute the kinematics of the index finger and the time-series of the elevation angles of the different body links. The absolute value of the jerk associated with the shoulder's marker was computed as the second derivative of its velocity absolute value, and it was used to quantify the smoothness of the movements.

Each elevation angle was defined as the angle between the corresponding body joint with respect to the vertical direction (Berret et al., 2009). The five elevation angles taken into consideration in this study were those relative to the shank (Sh), thigh (Th), trunk (Tr), humerus (Hu) and forearm (Fo). Elevation angles of the feet and head segments were not computed as they were not considered relevant for the analysis. Other standard kinematic parameters were calculated for both the index finger and the CoM: peak velocity (PV), mean velocity (MV), relative time to peak velocity (TPV) defined as the ratio of the duration of acceleration and MD, index of path curvature (IPC = Dev/LD) defined as the ratio of the maximum path deviation (Dev) from a straight line connecting the initial and final finger or CoM positions (linear distance, LD), and curvilinear distance (CD) defined by the integral over time from 0 to MD of the norm of the finger or CoM velocity vector in the sagittal plane. The smoothness of the movement was quantified by computing the maximum peak-to-peak value associated with the jerk of the shoulder marker (and it was indicated with JPP). All the kinematic variables associated with each single trial and single subject were time-interpolated to fit a standard 200-point time base. For both G and R movements, the time instants t_0, t_f and t_{pv} were computed for each trial: t_0 corresponded to the movement onset, at which the velocity profile of the right index finger exceeded 5% of its peak value; t_f , the end of the movement, was defined as the instant at which the index finger velocity profile dropped below 5% of its peak value (reached at instant t_{pv}). Movement duration (MD) was defined as the time interval between t_0 and t_f . For the EMG treatment and analysis we followed the same procedures described in Chiovetto et al. (2010). Briefly, muscle signals were full-wave rectified, normalized in amplitude with respect to their maximum value recorded across all trials and conditions and low-pass filtered with a zero-lag Butterworth filter and a cut-off frequency of 10 Hz. In in order to compute the average muscle activity across trials and subjects, the EMG signals comprised between 300 ms before t_0 and 100 ms after the end of the movement were normalized to a standard time window of 200

samples. Surface EMG electrodes were attached on each muscle by following standard recommendations and procedures, as indicated by Hermens et al., (2000). Nevertheless, contamination of the EMG muscle signals by the activations of other adjacent muscles could be possible and the amount of such contamination had to be assessed. Cross-correlation analysis between channels revealed that the average peaks of the cross-correlation function in an interval about lag zero never exceeded 0.3. Because of the difficulty of distinguishing between muscle crosstalk and synchronous recruitment of motor units in different muscles (d'Avella et al., 2008; Kilner et al., 2002) we did not excluded such muscles from further analyses. Thus, we verified that results obtained by working on different subsets of data in which muscle potentially affected by crosstalk were removed did not change significantly. Finally, we tested the absence of muscle cross-talk also by providing a small control experiment in one single subject. We provided electrical stimulation to the RF muscle of his right leg and recorded the activities of the VL and VM, which are muscles adjacent to the RF and could be the main locus of crosstalk effect. After stimulation, only RF presented clear muscle activation induced by the electric impulse, while for VL and VM no activity was recorded. This observation confirmed that the effect of muscle cross-talk on the global muscle activity could be considered minimal and negligible. Some among the twenty-four muscles recorded during the experiment for every participant showed a change in signal amplitude, because of the imperfect adhesion of the electrodes to the skin. These muscles were excluded from further analyses. The muscles that were eventually considered for analysis for each subject that participated to the experiment are listed in table 1.

Principal Component Analysis (PCA) and Non-Negative Matrix Factorization (NNMF)

PCA was applied, for each single condition, to the kinematic data describing the temporal evolutions of the elevation angles associated with each trial and subject. Because of the large differences of

magnitude between angular displacements of the upper versus lower-body joints, PCA based on the correlation matrix was performed. This choice was equivalent to operating an amplitude normalization of the joint displacements, so as to avoid biases in the analysis introduced by the joint displacements with the largest excursions. The number of PCs considered suitable to obtain a good compromise between the goodness of signal reconstruction and the level of physical interpretation of the solution was set according to an objective criterion: after examining the data reconstruction performance (expressed in percentage of variance accounted for) in function of increasing numbers of PCs, only the minimum number of PCs that could explain together at least the 90% of the total variation associated with the original data set (Berret et al., 2009; Thomas et al., 2005) was considered. The loadings relative to such PCs were analyzed to understand how variability of the angular displacements was captured by each PC.

PCA was also used to remove the intrinsic noise of measure affecting the EMGs. To this aim, PCA was applied to EMGs and the cumulative percentage of variance accounted for was again computed as a function of the number of PCs considered. The dimensionality D of the dataset was determined according to the 90% criterion mentioned above. EMGs were finally reconstructed and freed of noise by using just the first D extracted PCs. To identify specific patterns of activation characterizing the different muscle datasets, de-noised EMGs were applied a customized version of the NNMF algorithm proposed by Lee and Seung (1999), and based on the minimization of the cost function below

$$E^2 = \sum_{k=1}^{T} \left|\left| \mathbf{m}(t_k) - \sum_{i=1}^{N} c_i(t_k)\mathbf{w}_i \right|\right|^2$$

subject to the constraints $0 \leq w_{ij}$, $c_i(t) \leq 1$ and where T is the total number of time samples, $\mathbf{m}(t_k)$ is a vector of M real numbers whose elements are the activations at the instant t_k of the muscles taken into consideration, the $c_i(t_k)$ ($i=1,2,..,N$) are the combination coefficients and the w_{ij} ($i = 1,2,..,.N$, $j = 1,2,...,M$) are the elements of the basic time-invariant vectors of muscle activations (or muscle patterns) $\mathbf{w}_i$. The number N of combination coefficients and muscle vectors was set equal to the dimension D provided by PCA performed over the EMGs data set under investigation. The reader can refer to Chiovetto et al. (2010) for additional details regarding the algorithm implementation and the benefits deriving from the combined use of PCA and NNMF in sequence. It is here enough to remind that, because of the positivity of the processed EMGs, application of NNMF can facilitate the interpretation of the results. In the next section we will present for simplicity only the results relative to NNMF applied to the ensemble-averaged (across trials and subjects) muscle activities of F and R movements with target positioned at long distance (D2). Robustness and invariance of such results with respect to the data sets considered were however tested by applying NNMF separately also to the F and R muscle activities associated with the single subjects. Afterwards comparisons were made with those obtained from the enable-averaged muscle activities. Such test comparisons confirmed that results remained always the same across both F (as already shown in Chiovetto et al., 2010) and R data sets.

Statistical analysis

Statistical differences between mean values of kinematic parameters associated with G and R movements and between corresponding kinematic parameters of the index finger and CoM within the same experimental condition were tested by means of paired t-tests. The level of significance at which

the null hypotheses were rejected was set at 5%. Normality of parametric distribution was tested (Kolmogorov-Smirnov test). Pearson correlation coefficient (R) was used to assess the level of shape similarity between pairs of kinematic trajectories, PCs or EMG components identified by NNMF.

Results

General kinematic features

Fig. 1 depicts, for each target distance, typical stick diagrams associated with both F and R movements. In all cases, marked displacements of CoM and finger trajectories are evident and both present curvilinear shapes. Their trajectories are qualitatively always straighter and more horizontal at the beginning (end) of the F (R) movements, that is when the subject is closer to the upright standing position. Mean values of the kinematic parameters are reported in table 2. For both distances, the peak velocity of the index finger and the CoM were higher during the F movements than R ($p << 0.001$) and their acceleration phase (described by the TPV index) was shorter during R ($p < 0.001$). Movement duration (MD) was significantly smaller when reaching the target than when returning back to the standing position ($p << 0.001$). For both target distances, the linear and curvilinear distances LD and CD associated with the index finger and the CoM trajectories in the sagittal plan were significantly shorter during F movements ($p << 0.001$), while the index of path curvature (IPC) was smaller ($p << 0.001$). Similarly, mean values of the time to peak velocity (TPV) were smaller ($p < 0.05$ when target was at D1 and $p << 0.001$ when it was at D2, for both CoM and index finger). In the tasks with highest equilibrium demand, therefore, high differences were found for a parameter describing either postural (when referred to the CoM) or pointing (when referred to the index finger) features. As expected, the computation of the jerk relative to the shoulder's marker computed starting from its velocity absolute

value revealed that F movements, which were faster that R movements, were much jerkier than R ($p << 0.001$).

In summary, remarkable differences between F and R movements were found. F movements were always faster and jerkier than the R ones, and their mean TPV values were always shorter (possibly because of the action of gravity). The index finger and CoM trajectories associated with R movements resulted longer and more curved compared to G movements. Different kinematic features characterized the index finger and the CoM motions during the same movement when strong equilibrium efforts were required during the task.

Elevation angles and PCA

The average time series of the five elevation angles relative to movements with target at short and long distance are reported in Fig. 2. Initially, before reaching the target, all angles are very small or close to zero as subjects stood in upright position. During F movements all the angles change so as to determine the flexion of legs, trunk and arms. Note the mirrored behaviour of the Th angle with respect to Sk and Tr, and the similar trend of Hu and Fo: the two angle associated with the arm on average assume almost the same values, meaning that the arms were mainly kept still and rotate about the shoulder joints. The average time series of the elevation angles describing the return movements were on average similar to those of the forward movements (in Fig. 2 the time series of the returning motion were vertically flipped). Such angular displacements corresponded to extension of all the body segments until reaching a final, upright standing position. PCA over the elevation angles revealed that, when the target was at D1, two principal components could account for more than 90% of the variance associated with both forward and return movements (PC1 more than 80% by itself, see Fig 3 top panel): consequently the components of higher order were excluded from the analysis. When the target

was positioned at D2, the co-variation among the different elevation angles increased. More in detail, although the VAF by the first two principal components together did not changed drastically with respect to the movements with target at D1, the contribution provided by PC1 increased notably (% of VAF by PC1 was higher than 90% for both forward and returning movements, see Fig. 3). Note that, within the movements with target at the same distance, the amount of VAF and its distribution among the first two principal components was the same for forward and returning movements. The mean values of the loadings associated with each PC are illustrated in the middle and lower parts of the Fig. 3, for each elevation angle. In PC1, segments of the lower-body (Sh, Th and Tr) were always tightly coupled, during both forward and returning movements and independently of target distance. The upper-body segments always relative to PC1 showed instead a different behaviour, dependent of the target distance. Hu and Fo were found not coupled to the lower-body segments when the target was at D1. At the contrary, they became tightly coupled to the lower-body segments when target was at long distance. The loadings of PC2 showed that, with target at D1, Sk and Hu were highly coupled during forward movement, whereas Sk and Fo were tightly covering when subject moved back to the initial standing position. When target was positions at D2, PC2 just described variability associated with Hu. The shapes of corresponding principal components associated with F and R movements were compared (Fig. 4). Although the percentage of variance explained by corresponding PCs was the same independently of the direction of motion indeed (Fig. 3A), their shape might reveal very different. This would also indicate different pattern of angular co-variation of the elevation angles during G with respect to R movements. The high values of the correlation coefficients reported in Fig. 4, however, indicated that elevation angles co-varied in a similar way regardless of the direction of movements. The biggest difference between corresponding PCs was a slight temporal lag of the PC relative to the R motion, always anticipating the one relative to G. Such a lag can be explained by the different role

played by gravity during the two movements, which results in lower TPV values of finger and CoM during R movements). PCA revealed therefore that the angular synergies at the base of the pattern of co-variation between the different body segments did not change dependently of the direction of motion: the only exceptions were the loadings of Hu and Fo associated with PC2 with target at D1.

Muscle activity and NNMF

In Fig.5 the ensemble-averaged muscle activities associated with F and R movements are plotted. Such muscle patterns refer to movement accomplished with target at D2. As in Chiovetto et al. (2010) indeed, target distance was not found to play a relevant role on the shape of muscle signals and therefore from now on results we will refer, with no loss of generality, to the movements in which the target was positioned at longest distance. In the left column (F movement) muscles show the well-known triphasic pattern already described in literature (Chiovetto et al. 2010). A clear anticipatory muscle activity characterized movement initiation prior to t_0. Deactivation of a group of postural muscles (Sol, BF, ST, ES and SM) was followed by the activation of another group of both lower-limb (Tib, Per, RF, OI) and upper-limb muscles (Serr, DA and Pect). Then, between t_0 and t_{pv} a further set of muscles activated that before either deactivated (Sol, BF, ST, SM) or started becoming active (Gast, VL, VM, Add L, GM, LD, DP and Bra). The second half of the movement, starting after t_{pv}, was characterized by a significant tonic activity and co-contraction that likely contributed to stiffen the body joints to counterbalance the gravity effect. The right column depicts the average muscle activity of R movements. In this case all muscles presented initially, as at the end of the F movements, a high level of tonic activity. Anticipatory changes, however, still interested the time period prior to t_0. Some postural muscles (such as Tib and RF) together with RA and some upper-limb muscles (Pect, LD, Serr, DA, DP and Tri) deactivated, while other lower-body and trunk muscles (Sol, Gast, VL, BF, VM, ST,

SM, SM, ES and GM) activated. Differently from the activity of F movements, the largest part of the muscles (with the exception of Sol) presented no significant bursts of activation in the time period between t_o ant t_{pv} but, rather, they were characterized by a deactivation profile that coincided with the natural continuation of the initiation phase starting prior to t_o. In the second half of the R movements then, muscles presented just a modest level of tonic activity or presented almost no level of activation at all (as in the case of Tib and DA). Note that in Fig. 5 the level of tonic activity at the end of F movement was equal, for each muscle, to the initial tonic activity associated with R movements. In the figure however they look different just because of a different scale of the vertical axes of the graphs. The upper limit of the vertical axis of each graph was indeed set equal to the maximum value assumed by the average EMG signal plotted in that graph.

Application of PCA to the average muscle activities of F and R movements presented in Fig. 5 revealed that, in both cases, three PCs could account for more than 90% of their variance. The results of NNMF applied to ensemble-averaged EMG activities freed of noise according to the procedure described in the methods section are shown in Fig. 6. The two panels at the top of the figure show the time course of the combination coefficients $c_i(t)$, $i=1,2,3$ (ordered according to the timing of their peaks) for both movements. The upper-left panel confirms the results already described in Chiovetto et al. (2010) for F movements. Each peak was found playing a dominant role in one of the three time phases associated with the movements (time period prior to t_o, period ranging between t_o ant t_{pv} and the time period that goes from t_{pv} until the end of the movements). The coefficients $c_1(t)$ was the one mainly responsible for the initiation phase, $c_2(t)$ to muscle deactivations in the first time phases and muscle activations in the second phase, and $c_3(t)$ contributed the most to the final co-contraction of all muscles in the third and last phase of the movement. The contribution of each coefficient to each time phase was not unique as conversely it might have been expected. In fact $c_1(t)$ contributed partly also to

the co-contraction phase, as well as $c_3(t)$, that activated between t_0 and t_{pv}, played a role also in the braking one. This sharing of multiple contributions from different components by each time phase determined consequently the level of the muscle activations in each one of the three vectors w_i (Fig. 6, bottom panel). The coefficients associated with the R movement are illustrated in top-right panel of figure 6. Differently from the F case, in this the contribution of each coefficient resulted slightly modified. Although the contribution of $c_1(t)$ to muscle activation during the first time phase and the major contribution of $c_3(t)$ to the muscle tonic activity at the end of the movements, $c_2(t)$ was not found in this case to contribute to muscle activations in the second phase of the movement anymore, but just to muscle deactivations in the time period preceding t_0.

In conclusion, EMG analysis extended previous results regarding the tri-dimensional and triphasic muscle organization of forward WBP movements. The existence of two distinct groups of muscle (agonists and antagonists, refer to Chiovetto et al. 2010 for their definitions) acting synergistically was confirmed also when accomplishing R movements, as well as a tri-dimensional organization of the electromyographic activity. Agonists and antagonists switched roles during the two movements, at least in the first phase of the movement: the role of the agonists indeed, that in F were responsible for movement initiation, was replaced by the action played by the antagonists in R movements. Differently from the antagonist muscles, however, agonists did not played a braking role in the time period between t_0 and t_{pv}, and some of them just maintained a level of non-void tonic activity at the end of the movement. Therefore, despite the muscle organization of R movements was found to be still characterized by a tri-dimensional organization like that associated with the F movements, no more three but two main time phases were found to describe the time course of muscle activations relative to R movements. In the first phase agonist muscles deactivated and antagonist activated to initiate the movement. After this phase no active action was provided by muscles, letting

gravity braking the movement “naturally”. At the end of the movement (second phase) some muscles kept a non-void level of tonic activity to stabilize posture.

Discussion

In this study we compared the kinematic and electromyographic features of a reverse WBP task, in which subjects had to move back to an initial upright standing position, to those associated with a standard WBP movement in which subjects had to point to a target located in front of them (Stapley et al. 1999; Pozzo et al. 2002; Berret et al. 2009; Chiovetto et al. 2010). To this aim, general kinematic parameters were computed for each movement and PCA was applied to the time series describing the temporal evolution of the elevation angles associated with all the body links during either F or R movements. The shape of the extracted principal components and the values of the relative combination coefficients were then compared. Non-negative matrix factorization was moreover applied to the EMG signals collected from a large number of body muscles to assess their modular organization. It was found that, although the mean values of a set of movement parameters differed significantly dependently on the direction of motion, the pattern of joint co-variation remained instead substantially the same. On average, the waveforms of all the elevation angles simply underwent a reversal in time during R movements with respect of the F movements. Muscle organization of the forward whole-body pointing tasks was found instead to be remarkably different with respect to that characterizing the reverse movements. Our results extend those reported by other previous studies (Grasso et al. 1998; Papaxantis et al. 1998) and provide evidence that, although the motor plans and motor programs associated with multi-joint opposite movements in the gravity field are different, at kinematic level they are equally translated in the same pattern of motor co-variation.

Asymmetries were found characterizing, dependently on the direction on motion, CoM and finger kinematic parameters, suggesting differences in the motor plans relative to F and R conditions. Such results confirm those from previous investigations and relative to other kinds of opposite movements. Similarly to what has been reported in this study, asymmetric hand path and velocity profiles were indeed found during the accomplishment of arm reaching movements in the sagittal plane (Atkenson and Hollerbach, 1985; Papaxanthis et al. 1998a,b,c; Pellegrini and Flanders, 1998; Papaxanthis et al., 2003). Moreover, always in agreement with our results, hand-path curvature was reported to be greater and hand velocity profile to have smaller acceleration duration during an upward movement with respect to a downward movement. Other studies in the literature compared the kinematic behaviour associated with even more complex reverse tasks than simple arm movements. The existence of kinematic asymmetries was for instance reported also for the case of sit-to-stand (STS) and back-to-sit (BTS) tasks (Mourey et al. 2000, Scholz et al. 2001, Kerr et al. 1997, Schenkman et al. 1990; Papaxanthis et al. 2003).

In contrast to the marked differences that we found distinguishing the motor plans of F and R movements, our results provide instead evidence for the existence of common patterns of motor co-variation at the kinematic level. This result is not obvious a priori. Because of the intrinsic redundancy characterizing the human body and the different mechanical and sensory contexts characterizing the two movements, different coordinative strategies might have been expected. Moreover, F and R movements are drastically different. The first one is indeed strongly target-oriented, while the second one is more a postural task. Thus, for instance, during F movements high inter-joint coordination (typically characterizing arm reaching) might have been expected. During R movements instead, when the main goal is to recover a stable upright posture, one might have expected a returning motion starting with the extension of the arms followed that of the other body segments (so as to reduce the

total body momentum and to keep the balance more easily). The reasons to believe that the strong co-variation in the joint space cannot be casual or due to task constraints (e.g. to the requirements for equilibrium maintenance, similar initial and final body configurations, similar velocities and relatively short pointing movements) are multiple. The easiest to put forward is that, because of the large number of degrees of freedom involved during body movement, the target could be reached in many different ways (e.g. with or without flexion of the knees, with or without trunk bending, by moving first the arms and then the trunk plus lower limbs etc.), as well as subjects might use different coordinative strategies during the pointing and backward motions. To test such a hypothesis we asked one subject to accomplish F and R movements by following well-specific instructions. One of them was, among the others, to reach the target and to get back to the initial standing position by first rotating the knees, followed by the hip and actually the arms. The subject never reported difficulties in accomplishing the constrained tasks, as well as he did not perceive them to be unnatural. PCA applied to the kinematic data associated with multiple movements of this kind revealed that joint coordination decreased remarkably, regardless of the direction of motion (Fig. 7). In comparison to the results displayed in Fig. 3, where one single PC could account for more the 90% of the variance, it is clear from Fig. 7 that three PCs were instead required to satisfy the 90% criterion for F movements with imposed kinematic strategy, two PCs for R movements. Moreover, the shapes of the first two PCs extracted resulted much different from those shown in Fig. 4, as demonstrated by the computation of the average R value ($R = 0.37$).

The notion of motor pattern is strictly linked to those movement components that are repetitive and stereotypical across several kinds of movement transformations. Motor patterns are moreover thought to be the result of the interaction between central and peripheral influences (biomechanical characteristics and sensory afferent activities). Similarly to our findings, Grasso and colleagues (1998)

showed that the kinematic pattern associated with the elevation angles of thigh, shank, ankle and foot was conserved across the reversal of gait direction, at the expense of a complete different pattern of electromyographic activity of the leg muscles. Like reversal of gait direction represents a special kind of movement transformation, the same can therefore hold for R with respect to the F whole-body movements. Our results, therefore, seems to extend those by Grasso and colleagues, at least because of the larger number of body-joints considered. Grasso argued that, in the case of locomotion, conservation of the motor pattern do not arise from biomechanical constraints but may instead reflect a behavioural goal achieved by the central network involved in the control of locomotion. Despite the different neural mechanisms underlying locomotion and pointing tasks therefore, such consideration might however be true also in the case of F and R movements.

The reasons why strong joint coupling is maintained also during R movement may be multiple. In their work, Berret and colleagues (2009) attributed the strong joint coordination during unconstrained F movements to multiple factors, such as passive mechanical effects (Ramos and Stark, 1990; Eng et al. 1992; Pozzo et al. 2001) or attractor dynamics (Mussa-Ivaldi et al. 1988; Mohan and Morasso, 2006). Another hypothesis is that joint coupling may be the results of the combination of a low number of muscle synergies. In a study on arm reaching in stroke patients for instance, Cheung et al. (2009) supported evidence according to which cortical signals from M1, premotor, supplementary areas or basal ganglia would function to select and activate fixed muscle synergies specified by the spinal or brainstem networks. The authors showed that the EMG activities recorded from both the unaffected and the stroke-affected arms of the patients were characterized by very similar synergistic organizations, despite differences in motor performance between the arms, in cerebral lesion sizes and locations between patients. Prior to this study, Chiovetto and colleagues (2010) already demonstrated that the electromyographic activity of a whole-body pointing task could be explained by the weighted

sum of three functional muscle synergies: one to initiate the movement, one to brake it and a third one to stabilize the final body posture. The authors could thus link together, in a hierarchical view of motor control, the joint coordination characterizing the investigated motor tasks with a basic triphasic muscle pattern having similarities with the control schema of single-joint flexion-extension. Such results were confirmed by this study, which in addition also provided knowledge about the muscle activity of the reverse movement. Again, a triphasic organization might have been expected. However, a tri-dimensional muscle organization was still found, but made of two instead of three time phases. For R movements indeed the braking phase was not found as it was likely replace by the braking action exerted by gravity and other passive mechanical effects. The change of the mechanical and sensory contexts resulted therefore in a reorganization of the muscle activity that, however, still can provide a reason for the strong joint coupling characterizing also R movements.

In conclusion, the present investigation revealed that, for the accomplishment of complex multi-joint movements carried out under different mechanical and sensory contexts due to the different contribution given by gravity to movement dynamics, the CNS relies on different motor plans and different motor programs. The explanation for the kinematic differences between F and R movements was provided by the EMG analysis, which proved that the gravitational force is included into the motor plan when accomplishing whole-body tasks and consequently modifies the processes controlling movement programming. However, the same coordinative structure was found at kinematic level, where the waveforms of all the elevation angles simply underwent a reversal in time during R movements with respect of the F movements. Additional studied needs therefore to be carried out in the future to clarify better why inter-joint coordination is a so peculiar feature characterizing movement generation.

Acknowledgements:

Dr. Chiovetto's research was partly supported by EU grant FP7-ICT-248311 (AMARSI).

References

Atkenson CG, Hollerbach JM (1985) Kinematic features of unrestrained vertical arm movements. J. Neurosci. 5: 2318–2330.

Berret B, Bonnetblanc F, Papaxanthis C, Pozzo T (2009) Modular control of pointing beyond arm's length. J Neurosci 29:191–205.

Cheung VC, Piron L, Agostini M, Silvoni S, Turolla A, Bizzi E (2009) Stability of muscle synergies for voluntary actions after cortical stroke in humans. Proc Natl Acad Sci U S A 106(46):19563–19568.

Chiovetto E, Berret B, Pozzo T (2010) Tri-dimensional and triphasic muscle organization of whole-body pointing movements. Neuroscience 170:1223-38.

d'Avella A, Fernandez L, Portone A, Lacquaniti F (2008) Modulation of phasic and tonic muscle synergies with reaching direction and speed. J Neurophysiol 100(3):1433-54.

Eng JJ, Winter DA, MacKinnon CD, Patla AE (1992) Interaction of the reactive moments and center of mass displacement for postural control during voluntary arm movements. Neurosci Res Commun 11:73– 80.

Kaminski TR (2007) The coupling between upper and lower extremity synergies during whole-body reaching. Gait Posture 26:256–262.

Kilner JM, Baker SN, Lemon RN (2002) A novel algorithm to remove electrical cross-talk between surface EMG recordings and its application to the measurement of short-term synchronisation in humans. J Physiol 538:919–930.

Grasso R, Bianchi L, Lacquaniti F (1998) Motor patterns for human gait: backward versus forward locomotion. J Neurophysiol 80:1868–1885.

Hermens HJ, Freriks B, Disselhorst-Klug C, Rau G (2000) Development of recommendations for SEMG sensors and sensor placement procedures. J Electromyogr Kinesiol 10: 361–374.

Kendall FP, McCreary EK, Provance P, Rodgers MM, Romani WA (2005) Muscles: Testing and Function with Posture and Pain. Baltimore, MD: Williams & Wilkins.

Kerr KM, White JA, Barr DA, Mollan RA (1997) Analysis of the sitstand- sit movement cycle in normal subjects. Clin Biomech 12:236–245.

Ivanenko YP, Poppele RE, Lacquaniti F (2004) Five basic muscle activation patterns account for muscle activity during human locomotion. J Physiol (Lond) 556:267–282.

Lee DD, Seung HS (1999) Learning the parts of objects by non-negative matrix factorization. Nature 401:788–791.

Lockhart DB, Ting LH (2004) Optimal sensorimotor transformations for balance. Nat Neurosci 10(10):1329-36.

Mohan V, Morasso P (2006) A forward/inverse motor controller for cognitive robotics. Lect Notes Comput Sci 4131:602– 611.

Mourey F, Grishin A, d'Athis P, Pozzo T, Stapley P (2000) Standing up from a chair as a dynamic equilibrium task: a comparisonbetween young and elderly subjects. J Gerontol A Biol SciMed Sci 55:425–431.

Morasso P (1981) Spatial control of arm movements. Exp. Brain Res. 42: 223–227.

Mussa Ivaldi FA, Morasso P, Zaccaria R (1998) Kinematic networks. A distributed model for representing and regularizing motor redundancy. Biol Cybern 60:1–16.

Papaxanthis C, Pozzo T, Stapley P (1998a) Effects of movement direction upon kinematic characteristics of vertical arm pointing movements in man. Neurosci Lett 253:103–106.

Papaxanthis C, Pozzo T, Popov K, McIntyre J (1998b) Hand trajectories of vertical arm movements in one-G and zero-G environments: Evidence for a central representation of gravitational force. Exp Brain Res 120:496–502.

Papaxanthis C, Pozzo T, Vinter A, Grishin A (1998c) The representation of gravitational force during drawing movements of the arm. Exp Brain Res 120:233–242.

Papaxanthis C, Dubost V, Pozzo T (2003) Similar planning strategies for whole-body and arm movements performed in the sagittal plane. Neuroscience 117(4):779-83.

Pellegrini JJ, Flanders M (1996) Force path curvature and conserved features of muscle activation. Exp Brain Res 110:80–90.

Polyakov F, Drori R, Ben-Shaul Y, Abeles M, Flash T (2009) A compact representation of drawing movements with sequences of parabolic primitives. PLoS Comput Biol.

Pozzo T, Ouamer M, Gentil C (2001) Simulating mechanical consequences of voluntary movement upon whole-body equilibrium: the arm-raising paradigm revisited. Biol Cybern 85:39–49.

Pozzo T, Stapley PJ, Papaxanthis C (2002) Coordination between equilibrium and hand trajectories during whole body pointing movements. Exp Brain Res 144:343–350.

Ramos CF, Stark LW (1990) Postural maintenance during fast forward bending: a model simulation experiment determines the “reduced trajectory”. Exp Brain Res 82:651– 657.

Schenkman M, Berger RA, Riley PO, Mann RW, Hodge WA (1990) Whole-body movements during rising to stand from sitting. Phys Ther 70:638–648.

Scholz JP, Reisman D, Schöner G (2001) Effects of varying task constraints on solutions to joint coordination in a sit-to-stand task. Exp Brain Res 141(4):485-500.

Soechting JF, Laquaniti F (1981) Invariant characteristics of a pointing movement in man. J. Neurosci. 1: 710–720.

Stapley PJ, Pozzo T, Cheron G, Grishin A (1999) Does the coordination between posture and movement during human whole-body reaching ensure center of mass stabilization? Exp Brain Res 129:134–146.

Thomas JS, Corcos DM, Hasan Z (2005) Kinematic and kinetic constraints on arm, trunk, and leg segments in target-reaching movements. J Neurophysiol 93:352–364.

Tresch MC (2007) A balanced view of motor control. Nat Neurosci 10(10):1227-8.

Winter D (1990) Biomechanics and motor control of human movement. New York:Wiley.

Captions

Figure 1: Typical stick diagrams of the task performed for the near (D1) and the distant (D2) target representing the F movement, from the initial standing position until the pointing of the target, and the R movement, from the initial pointing position to the final standing position. The solid lines (green for the F and orange for the R) represents the finger trajectories, the dash-dotted ones those of the CoM.

Figure 2: Average time series of the five elevation angles. In each graph, time-series of the F (in green) and R movements (in orange) are reported. The graphs on the left refer to movements with target at distance D1. The graphs on the right refer to movements with target at distance D2. The small histograms report, for each elevation angles, the mean values (± SDs) of the peak-to-peak angular displacements.

Figure 3: On the top of the figure, the percentages of VAF by the first two principal components computed for the elevation angles, for the two target distances (D1, left histograms; D2, right histograms) and for the F and the R movements are shown. Below the two top histograms, the corresponding mean values (± SD) of loadings are presented.

Figure 4: The temporal shapes of the first two principle components are compared across movement directions. PCs referring to both F and R movements are illustrated for each target distance. R values of the correlation coefficients assessing the level of shape similarity between the pair of waveforms in each graph are reported.

Figure 5: Ensemble-averaged activity patterns of F (left column) and R (right column) movements. Muscle activities were obtained by averaging the muscle activations of all subjects and trials. At the top of each column the average index finger velocity profile is displayed.

Figure 6: Time courses of the average index finger velocity profiles of F (top-left panel) and R (top-right panel) movements and the corresponding combination coefficients $c_1(t)$, $c_2(t)$ and $c_3(t)$ extracted with NNMF from the ensemble-averaged EMG activity of Fig. 5 are shown. Muscle vectors associated with the corresponding combination coefficients of two above panels are also depicted (in the lowest part of the figure). Green indicates F movement, orange F indicates R movements.

Figure 7: The figure displays the percentages of VAF by the first three principal components computed from the elevation angles of the F and R movements when kinematic strategy was imposed. The subject was instructed to rotate sequentially the knees first, followed by hip and arms.

Table 2: The parameters included in the table are the following: peak velocity (PV), relative time to peak velocity (TPV), mean velocity (MV), movement duration (MD), curvilinear distance (CD), linear distance (LD), index of path curvature (IPC) and maximum peak-to-peak amplitude of the jerk (JPP).

D1

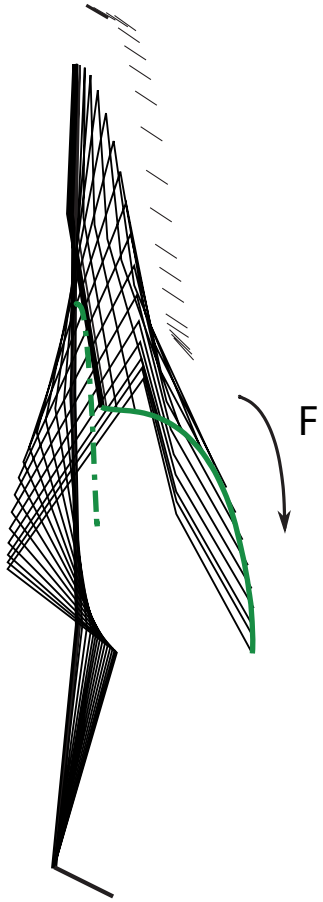

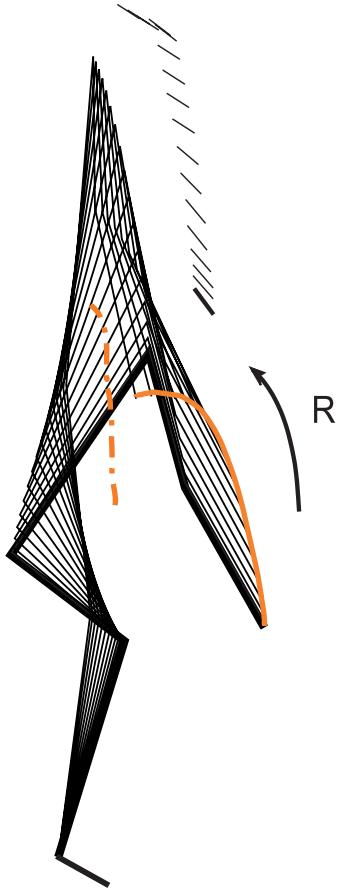

D2

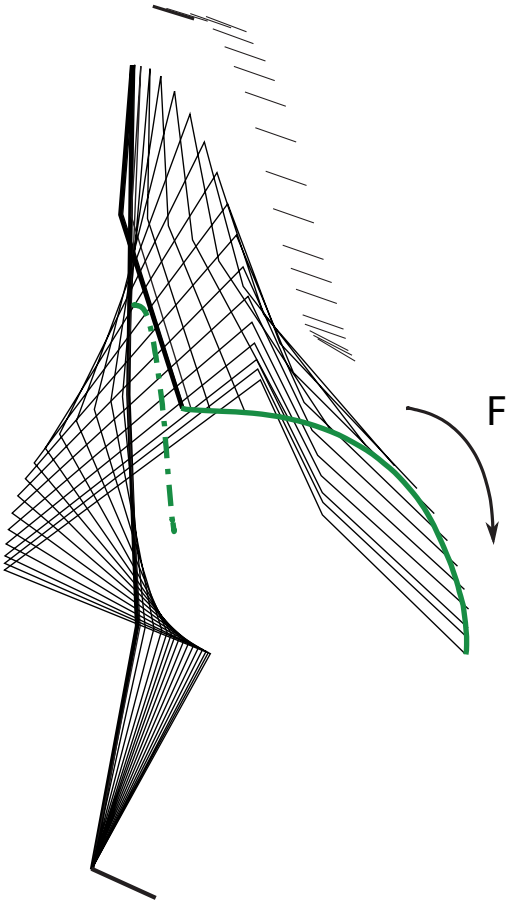

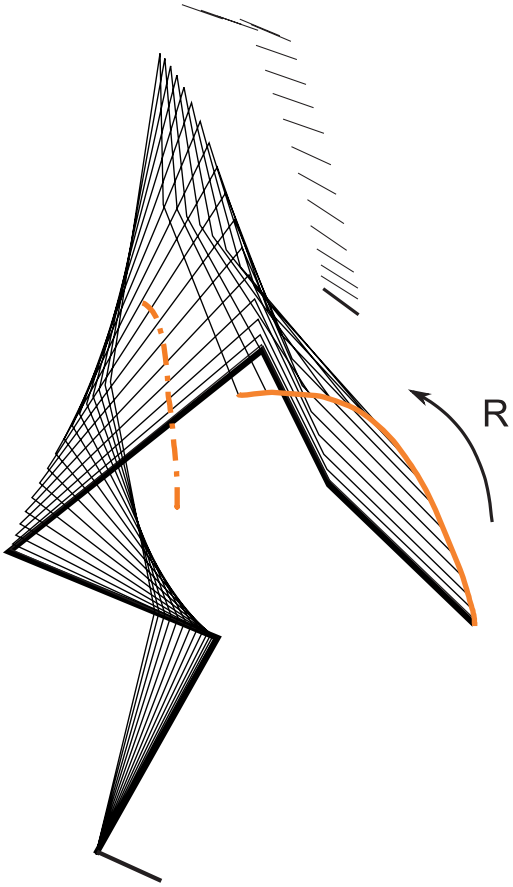

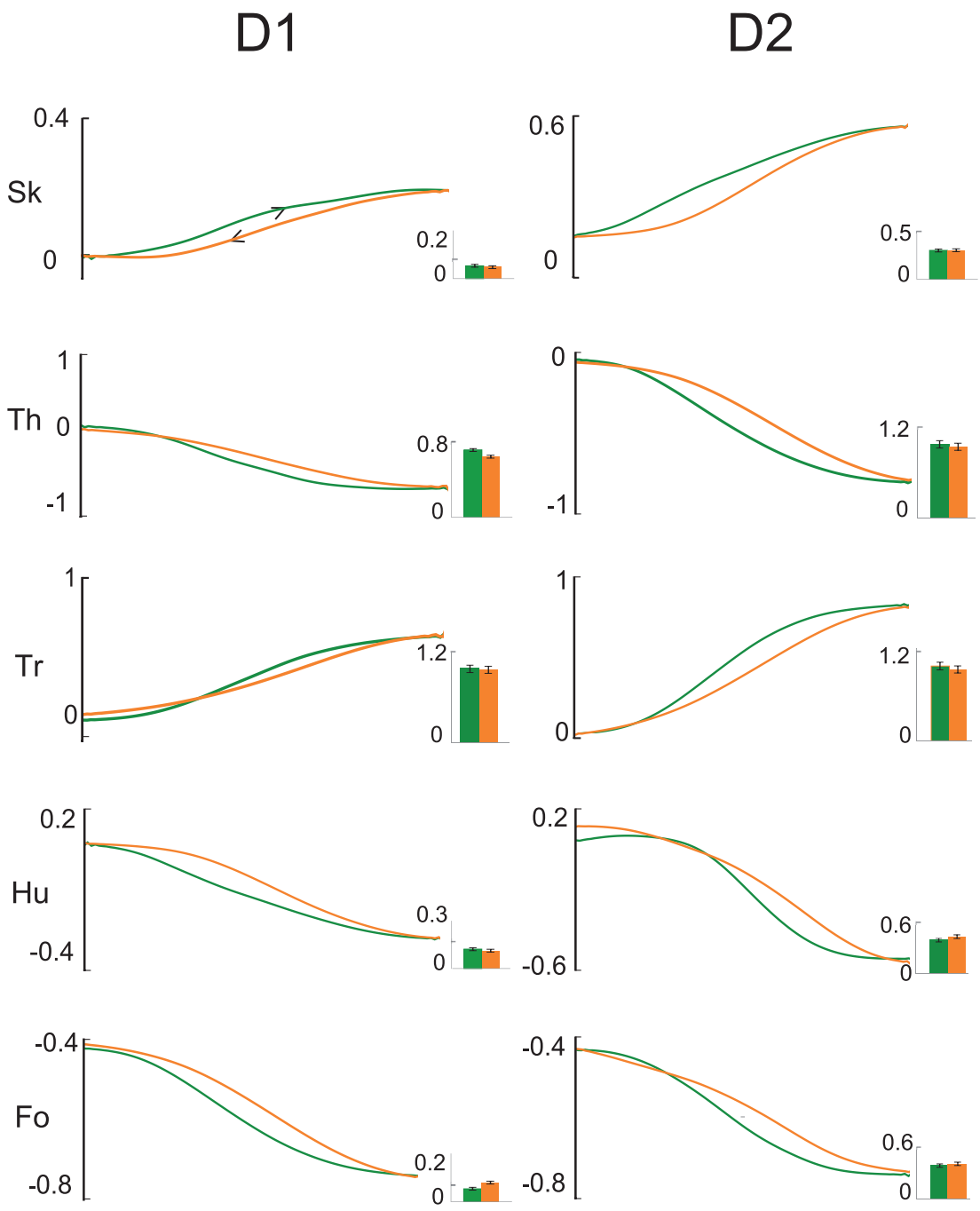
D1
D2
Sk
Th
Tr
Hu
Fo
0.4
0
0.2
0
0.6
0
0.5
0
1
0
-1
0.8
0
0
-1
1.2
0
1
0
1.2
0
1
0
1.2
0
0.2
-0.4
0.3
0
0.2
-0.6
0.6
0
-0.4
-0.8
0.2
0
-0.4
-0.8
0.6
0

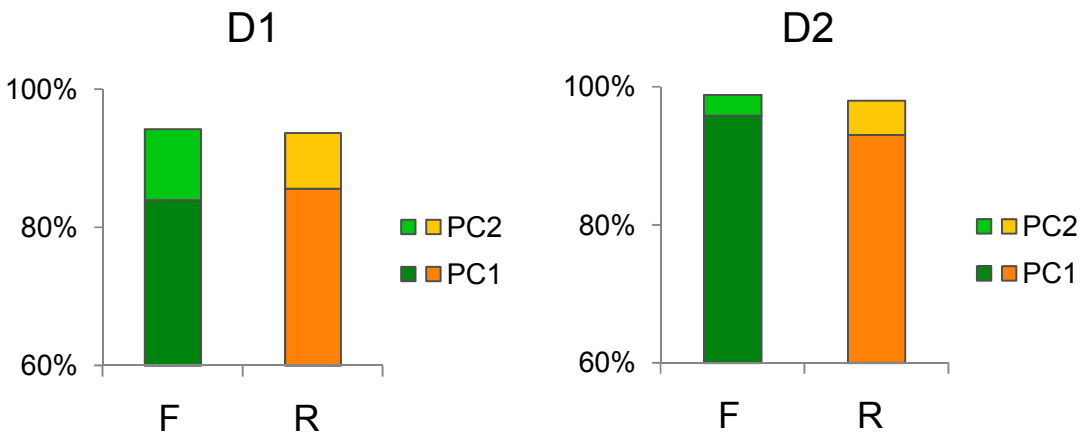

Loadings

D1

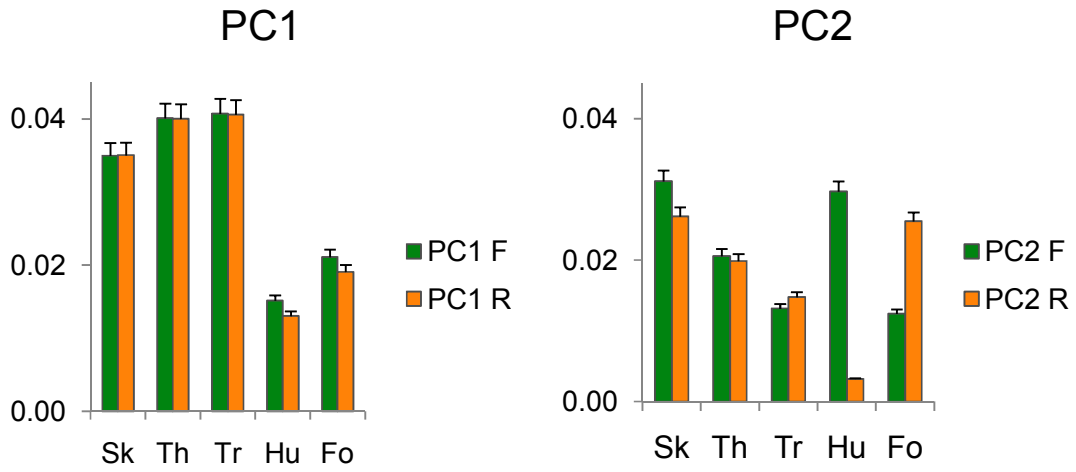

D2

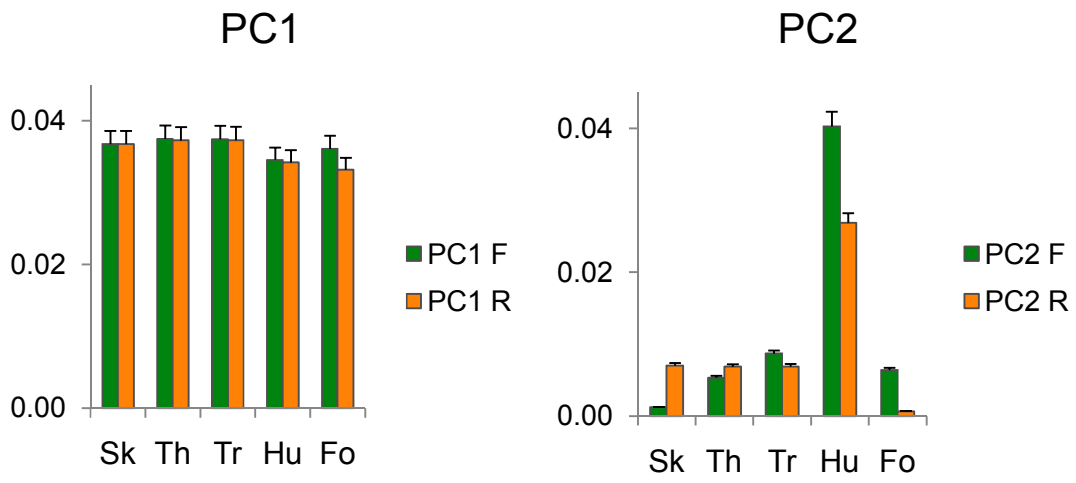

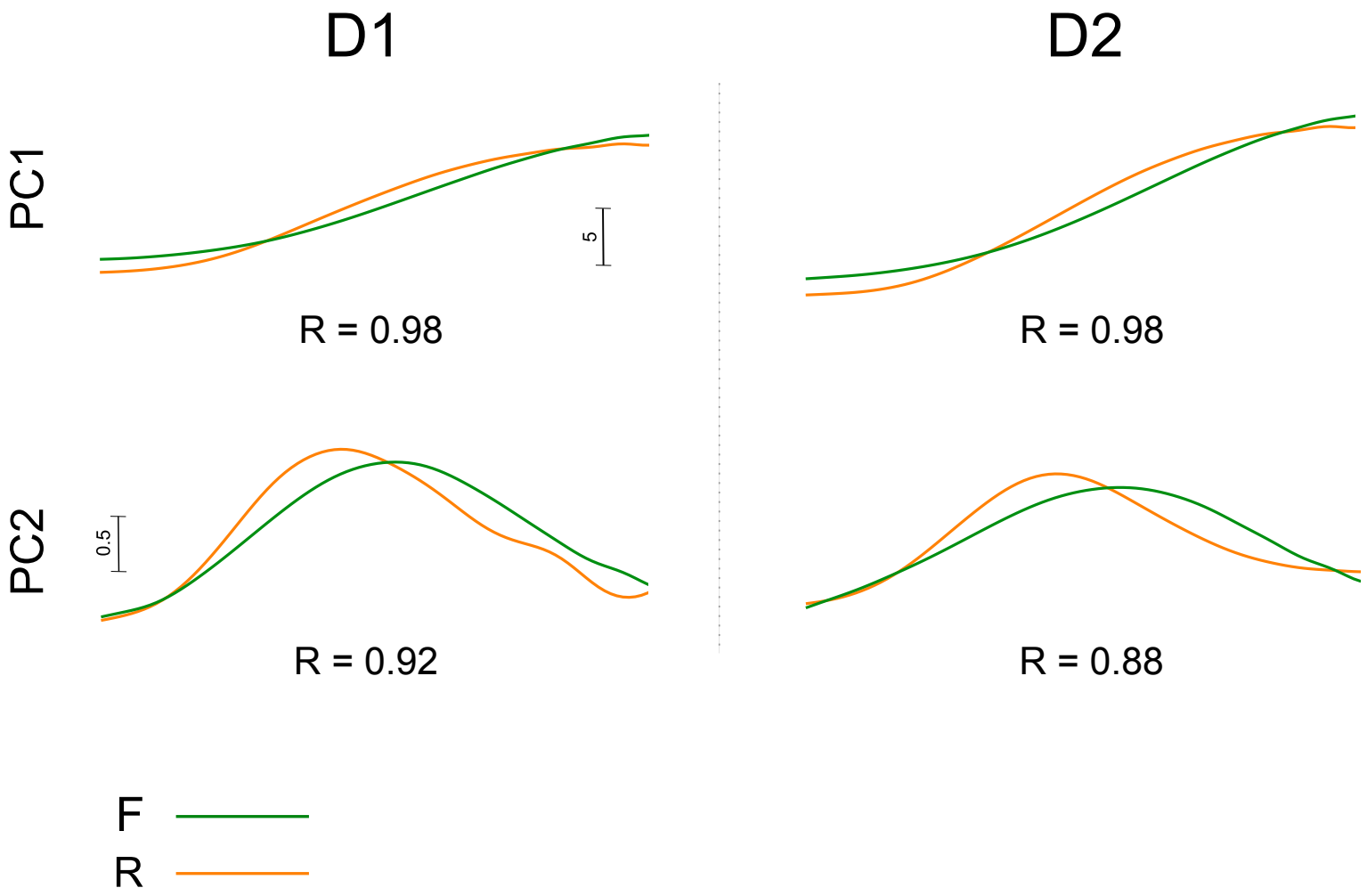
D1
D2
PC1
PC2
5
0.5
R = 0.98
R = 0.98
R = 0.92
R = 0.88
F
R

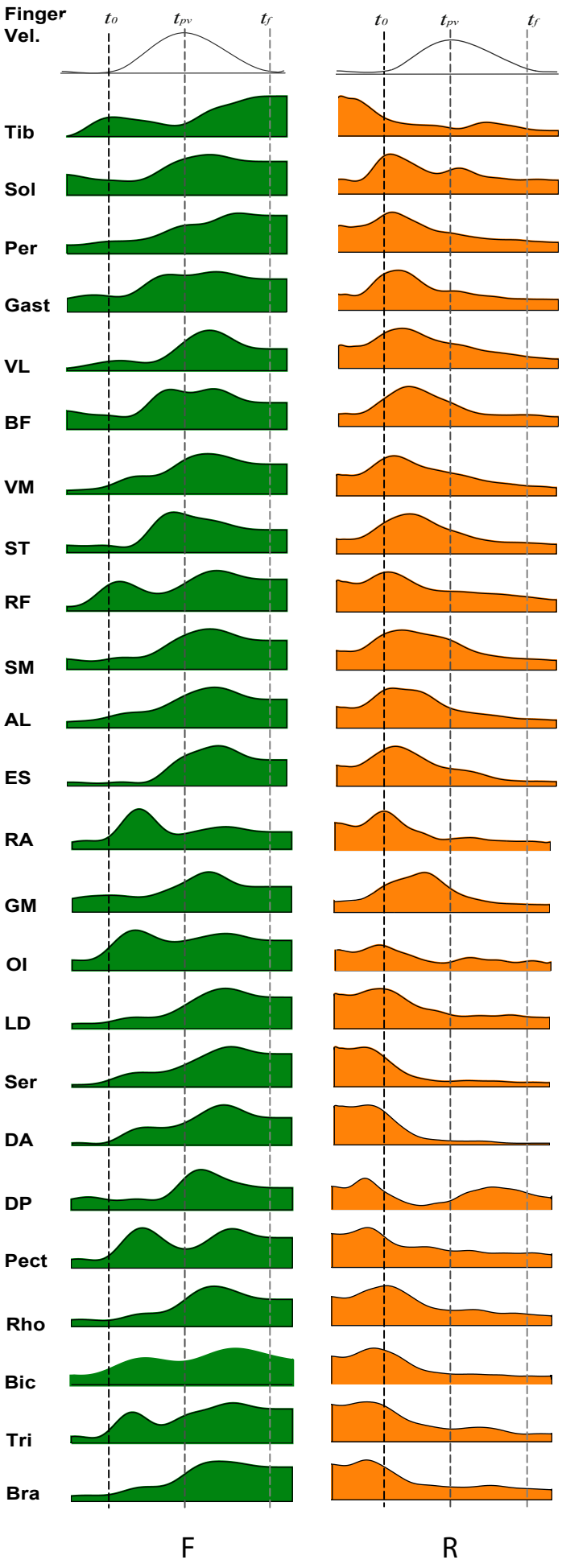
Finger Vel.
t_0
t_{pv}
t_f
t_0
t_{pv}
t_f
Tib
Sol
Per
Gast
VL
BF
VM
ST
RF
SM
AL
ES
RA
GM
OI
LD
Ser
DA
DP
Pect
Rho
Bic
Tri
Bra
F
R

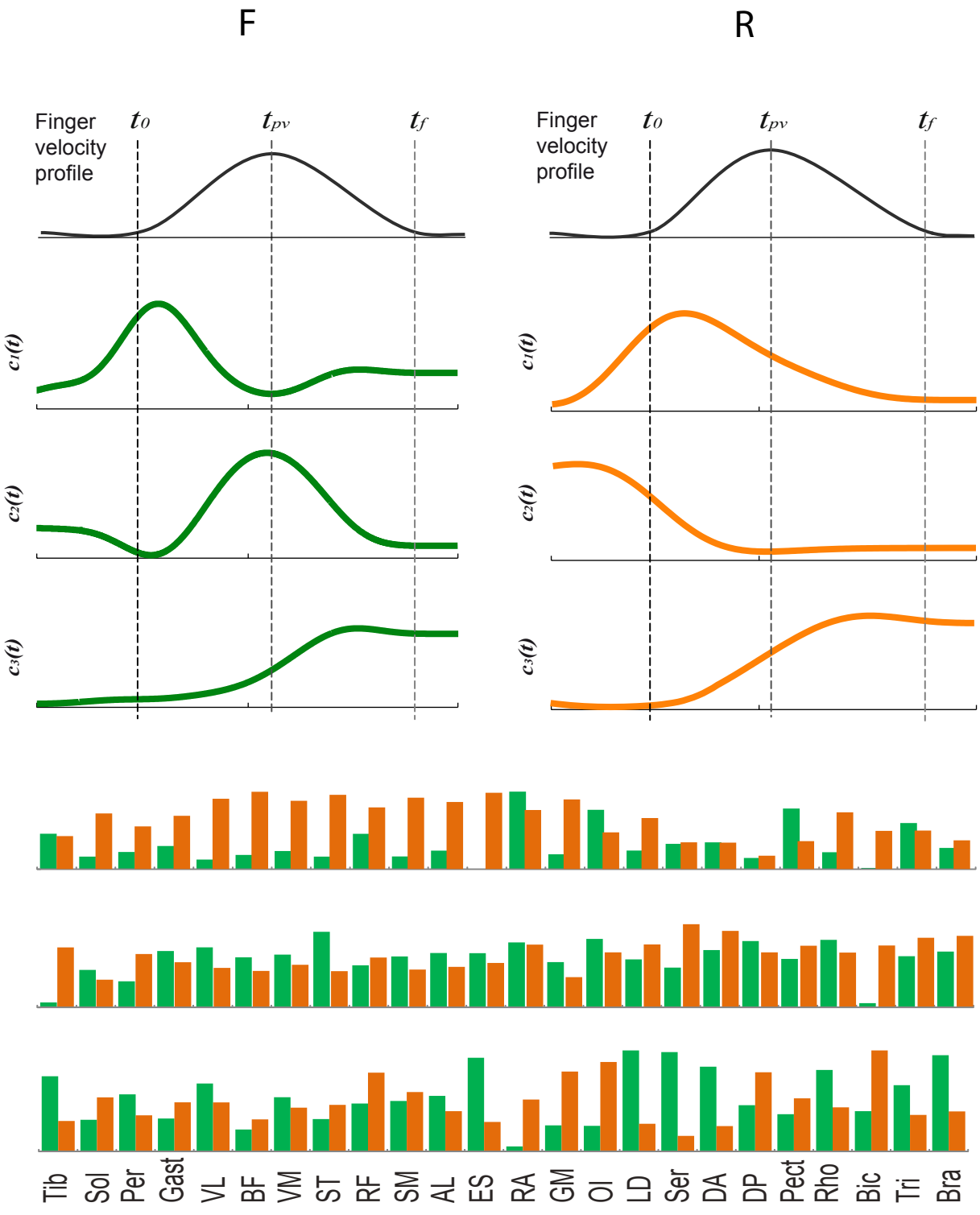
F
R
Finger velocity profile
t_0
t_{pv}
t_f
$c_1(t)$
$c_2(t)$
$c_3(t)$
Tib
Sol
Per
Gast
VL
BF
VM
ST
RF
SM
AL
ES
RA
GM
OI
LD
Ser
DA
DP
Pect
Rho
Bic
Tri
Bra

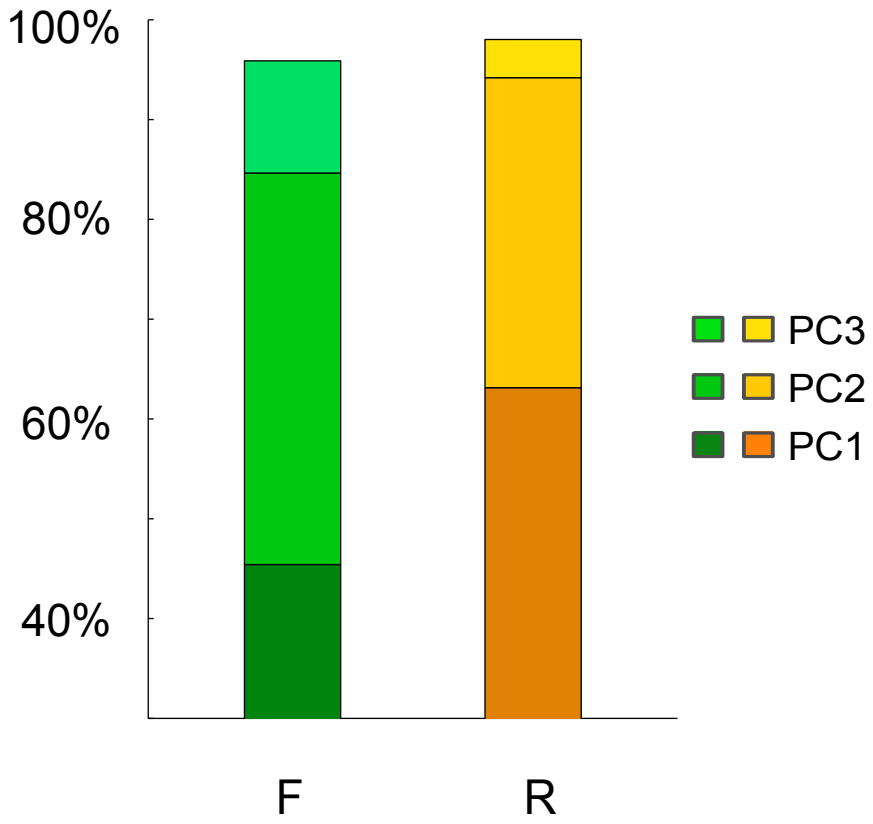
100%
80%
60%
40%
F
R
PC3
PC2
PC1